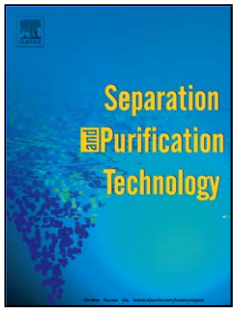

Title: Influence of exchanged cations (Na^+, Cs^+, Sr^{2+}, Ba^{2+}) on xylene permeation through ZSM-5/SS tubular membranes

Authors: Ana M. Tarditi, E.A. Lombardo

PII: S1383-5866(07)00477-7
DOI: doi:10.1016/j.seppur.2007.10.008
Reference: SEPPUR 9070

To appear in: *Separation and Purification Technology*

Received date: 31-7-2007
Revised date: 11-10-2007
Accepted date: 12-10-2007

Please cite this article as: A.M. Tarditi, E.A. Lombardo, Influence of exchanged cations (Na^+, Cs^+, Sr^{2+}, Ba^{2+}) on xylene permeation through ZSM-5/SS tubular membranes, *Separation and Purification Technology* (2007), doi:10.1016/j.seppur.2007.10.008

Influence of exchanged cations (Na^{+}, Cs^{+}, Sr^{2+}, Ba^{2+}) on xylene permeation through ZSM-5/SS tubular membranes

Ana M. Tarditi, E. A. Lombardo*

Instituto de Investigaciones en Catálisis y Petroquímica (FIQ, UNL-CONICET),

Santiago del Estero 2829, 3000 Santa Fe, Argentina

* Corresponding author: Tel.: +54 342 4536861

E-mail address: nfisico@fiqus.unl.edu.ar (E. A. Lombardo)

Abstract

Na-ZSM-5 membranes were synthesized by secondary growth on the outer surface of stainless steel porous tubes. The membranes were ion-exchanged with Cs^{+}, Ba^{2+} and Sr^{2+} to investigate their effect upon the separation of *p*-xylene from *m*-xylene and *o*-xylene. The permeation through the membranes was measured between 150 and 400 ºC using each xylene isomer separately and a ternary mixture. All the membranes were selective to *p*-xylene in the temperature range studied. N_2 and xylene permeation measurements together with SEM observations were used to determine whether or not cracks and/or pinholes developed after exposure to the xylene isomers at high temperature (400 ºC). Neither pore blockage nor extra-zeolitic pores developed after the ion exchange procedure and subsequent calcination. Furthermore, duplicate synthesized membranes of each cation form had similar separation factors and permeances. The duplicate values differ much less than the measurement error. The *p*-xylene permeation flux decreased in the order: Na-ZSM-5 > Ba-ZSM-5 > Sr-ZSM-5 ≅ Cs-ZSM-5 while the permeation flux of the *m*- and *o*-xylene decreased in the order Na-ZSM-5 > Sr-ZSM-5 > Ba-ZSM-5 > Cs-ZSM-5. The membrane that exhibited the best performance was Ba-ZSM-5, with a maximum p/o separation factor of 8.4 and a *p*-xylene permeance of 0.54 x 10^{-7} mol $s^{-1}m^{-2}$ Pa^{-1} at 400°C.

Keywords: Xylene isomers separation; ion-exchange effect; metallic tubular support; composite zeolite membranes.

1. Introduction

Interest in zeolite membranes has increased in the last few years due to their potential application to a wide range of gas/liquid separations, difficult to achieve by conventional techniques. Since the size of the zeolite pores is similar to the molecular dimensions, both selective adsorption and molecular sieving play important roles in the separation of hydrocarbon mixtures through this type of materials. In addition, these structures are thermally stable and resistant to aggressive environments, two very attractive features for petrochemical industry applications.

MFI-type zeolitic membranes (e.g., silicalite and ZSM-5) are able to separate mixtures of molecules with similar physical properties such as chemical isomers. Accordingly, significant efforts are being made to modify these membranes in order to improve their separation performance. Several groups have reported various results on the separation of xylene isomers using MFI-type zeolite membranes synthesized under different conditions [1-5]. The MFI-type structure has a three-dimensional pore system with straight channels in the *b*-direction (0.54 nm × 0.56 nm), interconnected with sinusoidal channels in the *a*-direction (0.51 nm × 0.55 nm). These pore sizes are close to the kinetic diameter of *p*-xylene (d_k = 0.58 nm), and it is expected that its bulkier isomers (*m*- and *o*-xylene, d_k = 0.68 nm) would diffuse at a significant slower rate through these pores. Thus, defect-free MFI zeolite membranes are expected to be capable of separating *p*-xylene from its isomers by shape-selectivity. However, literature results of xylene separation with MFI zeolite membranes present serious discrepancies which are mainly due to differences in membrane microstructure, material chemistry, and operational conditions.

Differences in chemical affinities, rather than shape or size with respect to the zeolite pore for the permeating molecules often determine the separation properties of

the zeolite membranes. One accessible way to modify the sorbent-sorbate interaction is through ion exchange. The affinity between zeolites and permeating molecules also plays an important role in the separation of adsorbing and non-adsorbing molecules. Based on these data, it could be predicted that permselectivity for mixed component systems is dependent on the interaction between permeates and pore walls as well as pore size. If a zeolite is ion-exchanged with cations which possess different interactions with permeates, this could improve the permselectivities of the membranes.

To this day, only a limited number of studies have been reported on permselectivities of ion-exchanged zeolite membranes. Jafer and Budd [6] used ion-exchanged NaA zeolite membranes with K^+ but observed no significant changes in pervaporation (isopropanol/water mixture) performance. Kusakabe et al. [7-9] studied the effect of different cations (Li^+, K^+, Mg^{2+}, Ca^{2+} and Ba^{2+}) on the performance of NaY membranes. CO_2 and N_2 single gas permeances were modified with these cations even though gas permeation rates and selectivities were not directly related to their size. Aoki et al. [10] studied the separation of butane isomers with ion-exchanged ZSM-5 zeolite membranes. In this study, the permeances decreased with increasing cation diameters (H^+, K^+, Ba^{2+}) but the n-C_4H_{10}/i-C_4H_{10} separation selectivities did not increase, even though the effective pore diameter apparently decreased.

The literature reports that *p*-xylene adsorbs selectively from a mixture of C_8 compounds on several zeolites. The selectivity for this isomer is strongly dependent upon the zeolite composition (Si/Al ratio and nature of the exchanged cation). The BaY zeolite is known to be selective for *p*-xylene, i.e., it preferentially adsorbs this molecule from a mixture of C_8 aromatics. Under the same conditions, the NaX zeolite is not selective. Both the adsorption of the molecules as well as their diffusion behavior contribute to the selectivity [11,12]. Adsorption and diffusion parameters play a key

role in the permeation mechanism of the xylene isomers through MFI zeolite membranes [2, 13]. Therefore, if the membranes are exchanged with different cations their performances will be modified. In a recent study [14], we reported a Na-ZSM-5 (Si/Al 100) composite tubular membrane with xylene permeances and separation factors equal to, or better than, other data reported for this geometry in the literature. However, it was also noticed that there was a strong need to improve the performance of the synthesized materials for practical applications. An easy way to modify the transport properties of the membrane was thought to be through ion exchange.

Another practical matter is to synthesize tubular composite membranes more amenable to industrial reactor applications. However, this geometry is more demanding than the flat disks, e.g. lower proportion of defects and higher selectivities are obtained with the latter type.

In this work, the single component and ternary mixture xylene permeation properties of the ZSM-5 exchanged membranes were studied. The membranes were synthesized in the outer surface of a stainless steel tubular support. The effect of different alkaline (Na^+, Cs^+), and alkaline earth (Ba^{2+}, Sr^{2+}) cations on the performance of the membranes was studied. In addition, the reproducibility of the synthesis method and ion-exchange procedure was verified. The membranes were characterized by XRD, SEM, EPMA, N_2 and xylene permeation measurements at temperatures between 150º and 400 ºC.

2. Experimental

2.1. Membrane preparation

Na-ZSM-5 membranes were synthesized using the secondary growth technique on the outer surface of a porous stainless steel (PSS) tubular support (Mott Metalurgical), 10 mm o.d. and 7 mm i.d. The average pore size was 0.2 μm. The

support was cut into 30-mm long pieces; then one end of the porous support was welded to a non-porous SS tube and the other end was sealed with a non-porous stopper. Through the open end, N_2 was injected to sweep the permeate. Before use, the tubes were ultrasonicated in acetone for 30 min. to remove organic contaminants and dirt. The ZSM-5 membranes were prepared by casting layers of silicalite seed crystals (ca. 250 nm). First, silicalite crystal seeds were synthesized under hydrothermal conditions in a Teflon-lined autoclave at a fixed temperature of 125 ºC for 8 h. The gel used to prepare the crystalline seeds contained Aerosil 300 as the Si source, tetra-propylammonium hydroxide (TPAOH) as the template, and NaOH as the mineralizing agent plus deionized water. The molar proportion was $25SiO_2$: 2.125NaOH: 6TPAOH: $333H_2O$ [15]. The seed suspension was then diluted by adding the water needed to yield a seed concentration of 20 g l^{-1}. The seeding was carried out as follows: the support was dipped in the colloidal solution and vertically withdrawn at a slow rate; then, it was dried for 30 min at room temperature and later, for 2 h at 90 ºC. This procedure was repeated twice.

The seeded supports were subsequently subjected to three hydrothermal reaction steps. The first one was conducted at 165 ºC for 8 h with a starting hydrogel having a Si/Al ratio of 100, using Aerosil 200 as the Si source, tetrapropylammonium bromide (TPABr) as the template, sodium hydroxide, deionized water and sodium aluminate as the Al source with the following composition: 21 SiO_2 : 1 TPABr : 3 NaOH : 0.105 Al_2O_3 : 987 H_2O [16]. The other two steps were performed with a starting hydrogel with a Si/Al ratio of 14, having a molar composition of 28 SiO_2 : 1,204 TPABr : 3,4 NaOH : 1 Al_2O_3 : 1288 H_2O [10]. In the latter two steps, Ludox AS 40 was used as the Si source.

After hydrothermal synthesis, the membranes were washed with deionized water, dried at 80 ºC for 24 h, and then tested for N_2 permeation. When the membranes were impermeable to N_2, the template in the zeolite pores was removed by heating in air at 470 ºC for 3 h with a heating rate of 0.3 ºC/min and a cooling rate of 0.5 ºC/min.

The cation exchange of the Na-ZSM-5 type zeolite membranes was carried out using alkaline (Cs^+) and alkaline earth (Ba^{2+}, Sr^{2+}) cations. The Na membranes were immersed in solutions of barium nitrate, strontium acetate, cesium acetate, at 80 ºC for 24 h. The cation concentration in each solution was 0.1 M. After the ion-exchange treatment, the tubes were thoroughly washed with distilled water and dried in air at ambient temperature for 2 h, and then at 80 °C for 24 h. In the case of the strontium exchanged membrane, two successive exchange steps were necessary to obtain the same extent of exchange as the Ba and Cs membranes. The powders obtained in the synthesis were exchanged under the same conditions in order to determine the extent of exchange by atomic absorption.

In order to verify the reproducibility of the synthesis method and the ion exchange procedure, duplicate membranes of different types were synthesized. Xylene permeation data were obtained for four different Na-ZSM-5 membranes. One of the Na-ZSM-5 (MM-11) membrane was obtained through the back-exchange of the Ba-ZSM-5 form (MM-11). To exchange all the Ba ions the membrane was tested twice with a 0.5 M solution of $NaNO_3$ at 80 ºC for 24h.

2.2. Physicochemical characterization

X-ray diffraction patterns of the membranes before and after exchange, the calcined membranes, and the residual powder collected at the bottom of the autoclave after synthesis were obtained with an XD-D1 Shimadzu instrument using Cu Kα

radiation at 30 kV and 40 mA. The scan rate was 1º min^{-1} in the 2θ=5-40º range. The XRD patterns of the membranes were obtained from smaller samples which were synthesized in the same vessel under the same conditions as the full size specimen. These samples were placed in the sample holder of the instrument.

The morphology of the membranes was observed by Scanning Electron Microscopy (SEM) using a JEOL JSM-35C instrument. The Si, Al, Fe, Ba, and Cs compositions were measured using an energy dispersive analytical system (EPMA) attached to the SEM instrument. The penetration of the zeolite layer in the micropores of the support was measured with SEM-EPMA.

The extent of ion exchange of the residual powder collected at the bottom of the autoclave after synthesis was determined through atomic absorption spectroscopy using a Perkin Elmer Analyst 800 instrument.

2.3. Permeation measurements

2.3.1. N_2 permeation

The N_2 permeation data was one of the criteria used to evaluate the extent of extra-zeolitic pores present in the membranes and the formation of a continuous film on top of the support surface. It was measured at 25 °C and a trans-membrane pressure of 80 kPa. The pressure difference across the membrane was controlled using a pressure regulator (Bronkhorst P-502C). All the permeation data are reported with a ± 95% confidence interval.

2.3.2. Permporosimetry

Permporosimetry measurements were made to estimate the contributions of zeolitic and non-zeolitic pores to the overall flux through the membranes. Nitrogen was

used as permanent gas and *p*-xylene as a condensable hydrocarbon. The experiments were performed at 25 ºC. The pressure difference through the membrane was kept at 60 kPa, while the permeate side was maintained at atmospheric pressure. At the beginning of the test, the N_2 permeance through the membrane was measured before introducing the xylene. This N_2 permeance at p/ps = 0 is the sum of the permeance through zeolitc pores and larger pores or defects. Then the permeance was measured at increasing p-xylene activity (p/ps from 0.025 to 1.0) to block the zeolite pores.

2.3.3. Xylene separation

The vapor permeation experiments were conducted using a shell-and-tube membrane module (Fig. 1). For these experiments, the membranes were connected to the permeation module using Teflon ferrules kept at temperatures lower than 200 ºC. Before testing, the MFI membranes were pre-treated at 300 °C under nitrogen flow for 2 h, then cooled to 150 ºC and kept at this temperature for another 4 h [3]. This treatment assured the desorption of gases that would affect the permeation measurements. The zeolite side of the tube was flushed with a N_2 carrier stream which previously passed through the xylene saturator maintained at 35 ºC, while the inside of the tube was flushed with N_2 as a sweep gas. The nitrogen feed flow rate and the sweep flow rate were set at 10 ml min^{-1} and 9 ml min^{-1} respectively, using mass flow controllers (MKS Instruments). The sweep gas flux of 9 ml min^{-1} is in the range where the permeation reaches a plateau with increasing N_2 flow rate. This was verified by experiments in which the sweep gas flow rate was varied between 5 and 40 ml min^{-1}. The total pressure at either side of the membrane was 1.013 x 10^5 Pa (1 atm). To prevent condensation of the organics and ensure correct xylene vapor pressure values, all system lines were kept at 150 ºC using heating tape.

The feed, permeate and retentate streams were analyzed with a Shimadzu GC-9A gas chromatograph equipped with a flame-ionization detector and a packed column containing Bentona 34 % and SP-1200 5% (Supelco). Single-gas and mixture tests were performed in the 150-400 °C range. The composition of the ternary mixture feed was 0.23 kPa *p*-xylene, 0.83 kPa *m*-xylene, 0.26 kPa *o*-xylene. This is the ratio of the thermodynamic equilibrium, composition of the isomers at 35 ºC. The single-component measurements were carried out with 2.026 kPa *p*-xylene, 1.92 kPa *m*-xylene and 1.52 kPa *o*-xylene. The experimental error in the molar fraction determination was less than 4%. The single-component permselectivity (ideal selectivity) was defined as the ratio of their fluxes, while the mixture separation factor was defined by the following equation:

$$\text{Separation factor} = \frac{\left(X_p / X_i\right)_{permeate}}{\left(X_p / X_i\right)_{feed}}$$

Where X_p represents mole fraction of *p*-xylene and X_i represents mole fraction of either *m*-xylene or *o*-xylene.

The catalytic inactivity of the membranes was confirmed by the results obtained during the permeation measurements made with each pure isomer up to 400 ºC. In these experiments, neither other isomers (including ethyl benzene) nor aromatics such as toluene or benzene were detected in the retentate or in the permeate side.

2.4. Adhesion of the zeolite layer to the support

In order to evaluate the adhesion of the synthesized membranes and determine the penetration of the zeolite layer inside the structure of the support, one of them was subjected to a different treatment. The membrane was sandpapered in several steps with

sandpaper number 800 and 1000, thoroughly washed with deionized water and then dried at 80 ºC for 24 h. After each sandpapering step, the membrane was tested for N_2 permeation and the weight loss was recorded.

3. Results

3.1. Synthesized composite membranes

Table 1 shows key features of the membranes. The third column indicates that the thickness of the membranes is fairly constant. The constancy of the permeation data before and after being in contact with the xylenes at 400ºC (4^{th} and 5^{th} columns) suggests that no cracks or pinholes have developed in the membranes after the high temperature cycles. The thermal stability of the composite materials will be confirmed by other observations (vide infra).

3.2. X-Ray Diffraction

The residual zeolite powder obtained from the hydrothermal syntheses with a hydrogel Si/Al ratio of 100 (first layer) and 14 (second and third layers) showed a well-defined MFI-structure as revealed by the presence of all its characteristic reflections (Fig. 2), which were not modified by calcination in air at 470 ºC. The clean diffractograms did not show any other zeolite structures nor the typical halo symptomatic of the presence of amorphous materials.

The XRD patterns show that all the membranes synthesized and calcined were composed of pure MFI zeolite, as revealed by the presence of its characteristic reflections between 2θ=7-9º and 2θ=23-25º (Fig. 3). The patterns were not modified by the ion-exchange process nor by the xylene permeation measurements (patterns not shown). In all the membranes, the crystals were randomly oriented since the relative

intensity ratios of the peaks were the same as those calculated from the reference powder diffractogram. These ratios were also very similar to those reported in the literature for randomly oriented membranes [17]. The lower signal to noise ratio of the diffractograms shown in Fig. 3 compared to those in Fig. 2 and the distortion of the patterns at low angles are due to the curvature of the tubular membrane.

3.3. Elemental composition

The elemental compositions of the residual zeolite powders obtained from the hydrothermal syntheses of the Na-ZSM-5 and after the ionic exchange (Cs^{+}, Sr^{2+}, Ba^{2+}) were obtained by atomic absorption while the compositions of the zeolite films were calculated from the EPMA data (Table 2). The M^{n+}/Al ratio was similar for the exchanged membranes, (taking into account that two monovalent and one divalent cation per two aluminum atoms are needed to balance the lattice charges). The thicknesses of the membranes obtained from the SEM micrographs are also shown in Table 2.

3.4. Morphology of the synthesized membranes

Fig. 4a shows the outer surface of the tubular support after coating with seed silicalite crystals. A high magnification was needed due to the small crystal size of the seeds. After the first hydrothermal synthesis, a layer with spherical crystals is formed on top of the support (Fig. 4b). It can be observed that the surface of the film (top view) after the third synthesis consists of tightly packed ZSM-5 crystals (Fig. 4c) with a good degree of intergrowth. Note that a continuous zeolite layer has been formed in spite of the surface roughness of the support. The zeolite layer ups and downs in some way mimic the support surface. A film with a randomly oriented structure was observed in

the SEM micrographs. This is consistent with the XRD patterns (Fig. 3). The first synthesis was made with a Si/Al ratio of 100 considering that when the syntheses are made directly with a Si/Al ratio of 14, the formation of a homogenous film on the surface of the support is impaired. It is known from the literature [16] that a high Al content decreases the zeolitization rate on the support, a possible solution being the growth of Al-rich films on top of Si-rich substrates, to help nucleation by providing an environment with a lower Al content. The SEM observations revealed that all the membranes synthesized presented the same morphology, which was not affected by ion-exchange (not shown).

The thicknesses of the membranes were measured in the SEM micrographs (Table 2). To obtain a representative estimate of those thickness five images were obtained at different points for each membrane. No precise determination of the thickness can be made, however, due to the unevenness of the support despite the fact that Fig 5a exhibits a relatively homogeneous and continuous film. This was achieved even in view of the difficulty in making a neat cut of the SS support. Fig. 5b presents the EPMA analysis data retrieved from the cross-section of one of the membranes. The zeolite film partially penetrates the pores of the support, consistent with the somewhat different weight gains of the membranes (Table 1). Note that the penetration of the zeolite inside the support is about 20 μm (from SEM-EPMA).

3.5. Permeation measurements

3.5.1. N_2 permeation

Before removal of the template, the membranes were impermeable to N_2 for a trans-membrane pressure of 80 kPa at room temperature. This means that the flow rate of N_2 was below the detection limits of our system (1×10^{-10} mol $s^{-1}Pa^{-1}$). The nitrogen

permeance increased substantially to the range of 10^{-8} mol s^{-1} m^{-2} Pa^{-1} after removal of the template. These values are in the range of those usually reported for good quality membranes synthesized on top of stainless steel supports [18, 19]. Table 1 shows the results of the single-gas permeation of nitrogen before the ion-exchange, and before and after the xylene permeation tests were conducted up to 400 °C. Note that the data obtained before the ion-exchange were reproducible for all the Na-ZSM-5 (Si/Al 14) membranes synthesized and the Ba-ZSM-5 composite back-exchanged with $NaNO_3$ (MM-11). The N_2 permeation of the membranes after the xylene measurements was similar to the data obtained before the ion-exchange (within the experimental error). It is important to note that neither the ion-exchange nor the xylene permeation measurements modified the nitrogen permeance data.

From the permporosimetry data it was possible to calculate that the contribution of non-zeolite pores to the total flux through the membranes was between 4.3 and 5% (Fig. 6). These data lend support to the validity of the exchanged cation effect upon the permeance and selectivity of ZSM-5 composite membranes. The permporosimetry data of membranes exchanged with each cation (Na, Sr, Ba and Cs) are shown in Figure 6. These data were obtained after xylene permeation measurements at 400ºC; those obtained with duplicate membranes (not shown) were in the same range as the membranes shown in Fig. 6 (between 4.3 and 5%).

3.5.2. Xylene permeation

Fig. 7 shows the xylene isomers ternary mixture permeation fluxes through the exchanged membranes. As shown in Fig. 7a the permeation fluxes of the three xylene isomers through the Na-ZSM-5 (MM-10) membrane increase with temperature but those of *m*-xylene and *o*-xylene are more pronounced. The membrane is selective to *p*-

xylene over the entire temperature range with a maximum p/o separation factor of 4.9 at 150 ºC. As the temperature increases, the selectivity decreases but the membrane is still selective for *p*-xylene at temperatures as high as 370 ºC, where the separation factors are p/o 3.75 and p/m 3.25.

For the Ba-ZSM-5 (MM-11) membrane, the *m*-xylene and *o*-xylene permeation fluxes in mixture increase with temperature while the *p*-xylene permeation flux slightly decreases (Fig. 7c). The decrease of the permeation flux with temperature can be attributed to the greater adsorption of *p*-xylene due to the presence of Ba^{2+} in the structure, as reported for other zeolite structures [12, 20-22]. This membrane has p/o and p/m separation factors of 13.6 and 8, respectively, at 150 °C. As the temperature increases, the separation factors decrease but the membrane is *p*-xylene selective at temperatures as high as 400 °C, where the separation factors are p/o 8.25 and p/m 6.

The other two membranes, Sr-ZSM-5 (MM-12) and Cs-ZSM-5 (MM-13) (Fig. 7b and d), exhibit the same tendency in the permeation fluxes of the xylene isomers with temperature as the Na-ZSM-5. The fluxes of the three xylene isomers are smaller than those obtained with all the Na and Ba-ZSM-5 membranes. These membranes are also selective to *p*-xylene in all the temperature range studied (150 and 400 ºC), but the separation factors are smaller than for the Ba-ZSM-5 membrane.

The permeation flux of different components through MFI type membranes as a function of temperature often exhibits a maximum at a certain temperature [23]. Sometimes a weak minimum is also observed at higher temperatures. These phenomena can be properly described by a combination of adsorption-diffusion processes. In the low temperature range, the permeation flux increases with temperature, driven by the increased mobility of adsorbed species, even though the amount of adsorbed material starts decreasing. Eventually, a maximum in permeation flux is reached, and above this

temperature the decline in occupancy prevails, which gives rise to a decrease in flux. At a certain temperature level, a local minimum is observed in the permeation curve. This corresponds to the point where adsorption effects become small enough so that the permeation is controlled by activated transport through the micropores, increasing monotonically with temperature. In a recent work Bernal et al. [24] showed that the position of the maximum and minimum in the permeation flux–temperature diagram can be used to rank adsorption effects in MFI membranes: a stronger adsorption would shift both the maximum and the minimum in the diagram towards higher temperatures.

As seen in Fig. 7, the *p*-xylene permeance flux for the Ba-ZSM-5 (MM-11) membrane decreases with temperature in the entire interval (150-400 ºC), but its minimum value is not even reached in the range explored, indicating a dominant influence of the adsorption process. The other membranes present a steady increase of the *p*-xylene fluxes with temperature; maybe these membranes exhibit a maximum and a minimum in the *p*-xylene flux at lower temperature. The above results may be symptomatic of a stronger adsorption effect.

The single components permeation fluxes of the xylene isomers and the ideal selectivities for the membranes, both at 370 ºC, are shown in Table 3. The Ba-ZSM-5 (MM-11) membrane again presents the best performance with a maximum p/o selectivity of 20.4 and p/m of 16.3 at 150 ºC. The difference in transport properties between single components and the ternary mixture is a consequence of the competitive adsorption-diffusion processes that occur in the latter case. For example, the presence of *p*-xylene in the mixture induces an increase in the pore size of the ZSM-5 structure [25] that facilitates the transport of the bulkier isomers with the consequent decrease in p/o and p/m separation factors.

In order to further confirm that the results obtained with the first series of composite membranes were due to the exchanged cations and not to random effects, duplicate Na^{+}, Sr^{2+} and Ba^{2+} membranes were assayed. Fig. 8 shows the separation factors and permeation fluxes at 370 ºC obtained with three Na, and two Sr and Ba-ZSM-5 composites. In addition, a Ba-ZSM-5 (MM-11) membrane was back-exchanged with $NaNO_3$ in order to further confirm that the cation exchange procedure does not affect the membrane quality as seen in Fig. 8a. Note the good reproducibility of the permeation flux data obtained in all cases. The small differences in the values obtained are well within the experimental error of the measurements. Besides, all the group of values obtained for each type of membrane are significantly different from each other. The behavior of the permeation flux of the three isomers with temperature was the same for duplicate membranes containing the same cation.

3.6. Adhesion of the zeolite layer to the support

Table 4 shows the data obtained along the adhesion stability test (N_2 permeance and weight loss after sandpapering the membrane). Note that with a weight loss of 64 % after the third erosion step, the N_2 permeance increased about 46 %. At this point, the naked-eye observation of the membrane showed the bright metallic surface of the support dotted with the opaque zeolite-filled pores. These data indicate that the zeolite material grown inside the pores affect the transport properties of the membrane.

4. Discussion

This study shows that the permeation fluxes of the xylenes and the separation factors are significantly affected by the nature of the cation which neutralizes the lattice charge of the ZSM-5. This statement is supported by both the reproducibility of the

synthesis method and the null effect of the ion exchange procedure upon the quality of the membranes. The exchanged zeolites show almost the same N_2 permeation at room temperature before and after membrane exposure to xylene mixtures up to 400 ºC: average N_2 permeance 5.8 ± 0.25 x 10^{-8} mol s^{-1} m^{-2} Pa^{-1} (calculated from Table 1). This is consistent with the invariance of the XRD patterns and the picture shown in the SEM micrographs, particularly seen in Fig. 4d. Furthermore, the duplicate synthesis of the membranes produced almost identical composites (Fig. 8). In Fig. 8a it is also shown that after back exchanging the Ba-ZSM-5 (MM-11) with $NaNO_3$ the recovered Na-ZSM-5 structure exhibits the same xylene permeation properties as the other Na containing membranes. All these features are indicative of the good reproducibility of the synthesis procedure and clearly indicate that either no pore blockage or pinhole appearance has occurred as a consequence of the ion exchange procedure. Besides, these results show the stability of the zeolite films after exposure to xylene mixtures up to 400 ºC.

In a previous work [14] we showed that the Na-ZSM-5 (Si/Al 100) membrane was stable for at least 1000 h on stream under the same conditions including three temperature cycles between 25 º and 400 ºC. The Na-ZSM-5 (Si/Al 14) membranes synthesized in this work were stable for about 800 h on stream. The main factor that plays a role in the stability of these membranes seems to be the penetration of the zeolite film inside the tube pores as shown by SEM-EPMA (Fig. 5) and the effect observed upon sandpapering the membrane (Table 4). This increased interaction might explain the resistance of these composite membranes to the thermal cycles despite the differences in expansion and contraction coefficients of stainless steel (10 - 19 x 10^{-6} $ºC^{-1}$) and ZSM-5 (-10^{-6} $ºC^{-1}$). On the other hand, the growth of the zeolite film inside the

pores negatively affects the permeation of the composite membrane (Table 4). There is, then, a trade-off between stability and permeance in this system.

The good quality of the tubular membranes was verified by permporosimetry data which showed that the non-zeolitic contribution to the total flux was between 4.3 and 5 % in the composites (Fig. 6). This is further confirmed by plotting the permeation fluxes of the three isomers as a function of the difference in pressure across the membrane between 10 and 65 kPa (data not shown). When ΔP approaches 40 kPa, a saturation value is reached in all cases. This is typical of zeolitic transport where the flow increases with the coverage up to a saturation value. This mechanism is modeled by the Maxwell-Stefan equation. If the transport through larger pores (Knudsen or viscous flow) were the dominant effect, the flow should show at least a linear increase with ΔP.

It is well known that the transport of hydrocarbons through the zeolite pores is controlled by a combined adsorption – diffusion mechanism. In the case of *m*- and *o*-xylenes diffusion is the predominant factor in all the synthesized membranes since:

i) The permeation fluxes increase with temperature (Figs. 7).

ii) They decrease with increasing cation radii (Table 5) and this indicates that the steric effect governs the permeation of these bulkier isomers (kinetic diameters 0.68 nm vs. 0.58 nm of *p*-xylene).

On the other hand, this is not the case of *p*-xylene where the adsorption phenomenon is more pronounced. In the cases of the Na, Cs and Sr-ZSM-5, the *p*-xylene adsorption diminishes the slopes of the permeation flux curves compared with those of the other isomers (Figs. 7a, b and d) while in Ba-ZSM-5, the permeation flux decreases slightly with temperature (Fig. 7c).

Note that the *p*-xylene flux of the membranes (Na-ZSM-5 > Ba-ZSM-5 > Sr-ZSM-5 > Cs-ZSM-5) did not decrease in the same order as the ionic radius increased ($Na^+ < Sr^{2+} < Ba^{2+} < Cs^+$). This is also reflected in the lack of correlation between either the ideal selectivity or the separation factors and the ionic radii (Fig. 9). This tendency is consistent with neither the decrease in the charge/radius ratio ($\Psi_i = z^*e/r$), $Sr^{2+} > Ba^{2+} > Na^+ > Cs^+$, nor with the Pauling electronegativity values (Table 5). The singular behavior of the permeation flux of *p*-xylene in the Ba-ZSM-5 membranes can be attributed to the greater adsorption when Ba^{2+} is present in the structure, as reported for other zeolite structures like BaY [12, 20-22]. Consequently, these are the most selective membranes in all the temperature range studied (between 150 and 400 ºC). Note in Fig. 9 that the separation factors and the ideal selectivities follow the same trend regardless of the cation involved. This is consistent with the known effect of pore expansion produced by *p*-xylene [25] that seems to be practically independent of the nature of the exchanged cation.

No transport data of xylenes across composite membranes made of Cs, Sr or Ba-ZSM-5 was found in the open literature. The situation is better in the case of silicalite and Na-ZSM-5. However, most of the reported data were obtained with flat membranes and very few using tubular supports. The cylindrical membranes show lower separation factors than the discs. This seems to be due to higher concentrations of defects that are generated on non-flat surfaces. Hedlund et al. [1] obtained permporosimetry data for their silicalite/α-Al_2O_3 flat membranes. They reported values between 1 and 24% for the fraction of non-zeolitic pores with separation factors varying between 16 and 1. They assigned this variation in the fraction of defects to the different synthesis methods they used. Relevant to our argument is that its membrane with 6% of defects had a separation factor of 3, similar to our Na-ZSM-5 (5% and 3.8). Tsapatsis and coworkers

reported [5] and patented [27] the best ZSM-5/α-alumina disk membrane to date, with no defects (undetectable by permporosimetry). At the maximum temperature they tested (220 ºC) the p/o separation factor was 381 average and a permeance of 1.91 x 10^{-7} mol s^{-1} m^{-2} Pa^{-1} average. The authors said [5] and we agreed that higher temperatures and pressures should be tested to ascertain the commercial feasibility of their membranes.

The tubular membranes are more useful than the flat disks, for practical applications such as a membrane reactor. This is why in Table 6, our data are mainly compared to those reported in the literature for cylindrical geometry. The much better performance reported for flat membranes is a sort of benchmark not yet reached in the open literature with tubular ones. Note that reference three is the only one that reports data obtained using a stainless steel tubular support. Fig. 10 presents a permeance-separation factor diagram. It shows results regarding MFI-type membranes performance found in the literature including the membranes synthesized in this study. Table 6 lists additional information of the tubular membranes presented in Fig. 10 plus the most relevant ones synthesized on disk supports.

Because of the potential use of these composites in a xylene isomerization membrane reactor, the required operation temperature is somewhere between 350º and 400ºC. Then, only the fourth entry in Table 6 is strictly comparable to ours. For this silicalite, although the p/o selectivity is good the permeation is about five times lower than those shown for Na- and Ba-ZSM-5.

In an earlier work, we reported data obtained with a Na-ZSM-5 membrane with a Si/Al 100 [14]. Comparing the present results with those we reported earlier, one can see two things: i) Ba-ZSM-5 (Si/Al 14) are the most selective membranes with a slightly lower permeance than Na-ZSM-5 (Si/Al 14) (compare data of rows 7 and 8), ii) Decreasing the Si/Al ratio from 100 to 14 increases the permeance while decreasing the

selectivity (see rows 6 and 7). The latter observation is consistent with the known fact that by increasing the aluminum content, the *p*-xylene adsorption diminishes.

5. Conclusions

The synthesis procedure used in this work yielded reproducible and durable composite membranes. The key factor that inhibits the appearance of pinholes and fractures during thermal cycles seems to be a certain degree of penetration of the zeolite phase (ca. 15 μm) inside the tube pores. In all the exchanged membranes 95-96% of the xylene transport occurred through zeolitic channels.

Out of the four cations exchanged, the Ba-ZSM-5 membranes were the best taking into account both permeation and selectivity. At 400ºC, the p/o separation factor was 8.4 and the *p*-xylene permeance 0.54 x 10^{-7} mol $s^{-1}m^{-2}$ Pa^{-1}. The better performance of these membranes is probably due to the stronger adsorption of *p*-xylene in barium containing zeolites than in the Na, Sr and Cs exchanged ZSM-5 films.

The permeation fluxes of the bulkier *m*- and *o*-xylene isomers decrease in the order Na-ZSM-5 > Sr-ZSM-5 > Ba-ZSM-5 > Cs-ZSM-5, in the same way as the ionic radio increases (Na^+ < Sr^{2+} < Ba^{2+} < Cs^+). A more complex adsorption-diffusion interaction dominates the *p*-xylene permeation behavior.

Acknowledgements

The authors wish to acknowledge the financial support received from UNL, CONICET and ANPCyT. Thanks are given to Elsa Grimaldi for the English language editing. A.M.T. thanks the YPF Foundation for the support received for her doctoral scholarship.

References

[1] J. Hedlund, F. Jareman, A-J. Bons, M. Anthonis, A masking technique for high quality MFI membranes, J. Membr. Sci. 222 (2003) 163 – 179.

[2] L. van Dyk, L. Lorenzen, S. Miachon, J.-A. Dalmon, Xylene isomerization in an extractor type catalytic membrane reactor, Catal. Today 104 (2005) 274 – 280.

[3] Ch. J. Gump, V. A. Tuan, R. D. Noble, J. L. Falconer, Aromatic permeation through crystalline molecular sieve membranes , Ind. Eng. Chem. Res. 40 (2001) 565 – 577.

[4] G. Xomeritakis, S. Nair, M. Tsapatsis, Transport properties of alumina-supported MFI membranes made by secondary (seeded) growth, Micropor. Mesopor. Mater. 38 (2000) 61 – 73.

[5] (a) Z. Lai, G. Bonilla, I. Díaz, J. G. Nery, K. M. A. Sujaoti, A. Amat, E. Kokkoli, O. Terasaki, R. Thompson, M. Tsapatsis, D. Vlachos, Microstuctural optimization of a zeolite membrane for organic vapor separation, Science, 300 (2003) 456 – 460. (b)Z. Lai, M. Tsapatsis, Gas and organic vapor permeation through b-oriented MFI membranes, Ind. Eng. Chem. Res., 43 (2004) 3000 – 3007.

[6] J.J. Jafer, P. M. Budd, S, Separation of alcohol/water mixtures by pervaporation through zeolite A membranes , Micropor. Mater. 12 (1997) 305 – 311.

[7] K. Kusakabe, S. Yoneshige, A. Murata, S. Morooka, Morphology and and gas permeance of ZSM-5-type zeolite membrane formed on a porous α-alumina support tube, J. Membr. Sci., 116 (1996) 39 – 46.

[8] K. Kusakabe, T. Kuroda, A. Murata, S. Morooka, Formation of a Y-type zeolite membrane on a porous-alumina tube for gas separation, Ind. Eng. Chem. Res. 36 (1997) 649 – 655.

[9] K. Kusakabe, T. Kuroda, K. Uchino, Y. Hasegawa, S. Morooka, Gas separation properties of ion-exchanged faujasite-type zeolite membranes, AIChE J. 45 (1999) 1220 – 1226.

[10] K. Aoki, V.A. Tuan, J.L. Falconer, R.D. Noble, Gas permeation properties of ion-exchanged ZSM-5 zeolite membranes, Micropor. .Mesopor. Mater. 39 (3) (2000) 485 – 492.

[11] H. Jovic, M. Bée, A. Méthivier, J. Combet, Influence of the cation composition on the dynamics of xylenes in X-type zeolites, Micropor. Mesopor. Mater. 42 (2001) 135 – 155.

[12] H. Jovic, A. Méthivier, G. Ethlers, Different diffusivities of xylene isomers in BaX zeolite measured by the neutron spin echo technique, Micropor. Mesopor. Mater. 56 (2002) 27 – 32.

[13] K. Keizer, A. J. Burggraaf, Z.A.E.P. Vroon, H. Verweij, Two component permeation through thin zeolite MFI membranes, J. Membr. Sci. 147 (1998) 159 – 172.

[14] A. M. Tarditi, G. Horowitz, E. A. Lombardo, A durable ZSM-5/SS composite tubular membrane for the selective separation of p-xylene from its isomers, J. Membr. Sci. 281 (2006) 692 – 699.

[15] M. A. Ulla, R. Mallada, J. Coronas, L. Gutierrez, E. Miró, J. Santamaría, Synthesis and characterization of ZSM-5 coating onto cordierite honeycomb supports, Appl. Catal, 253 (2003) 257 – 269.

[16] J. Coronas, J. L. Falconer, R. D. Noble, Preparation, characterization and permeation properties of tubular ZSM-5 composite membranes, AIChE J., 43 (1997) 1797 – 1812.

[17] Ôhrman, O., Hedlund, J., Synthesis and catalytic evaluation of zoned MFI films, Micropor. .Mesopor. Mater., 91 (2006) 312 – 320.

[18] C. Algieri, P. Bernal, G. Goléeme, G. Barbieri, E. Drioli, Permeation properties of a thin silicalite-1 (MFI) membrane, J. Membr. Sci. 222 (2003) 181 – 190.

[19] V. Sebastián, I. Kumakiri, R. Bredesen, M. Menéndez. Zeolite membrane for CO_2 removal: Operating at high pressure, J. Membr. Sci. 292 (2007) 92 – 97.

[20] R.R. Poissant. Y. Huang, R. A. Secco, A study of the sorbate-sorbent interaction in xylene/zeolite Y systems by FT-Raman spectroscopy, Micropor. Mesopor. Mater. 74 (2004) 231 – 238.

[21] J-P. Bellat, M.-H. Simonot-Grange, S. Jullian, Adsorption of gaseous *p*-xylene and m-xylene on NaY, KY, and BaY zeolites: Part 1: Adsorption equilibria of pure xylenes, Zeolites 15 (1995) 124 – 130.

[22] J-P. Bellat, M and M-H. Simonot-Grange, Adsorption of gaseous *p*-xylene and m-xylene on NaY, KY, and BaY zeolites: Part 2: Modeling. Enthalpies and entropies of adsorption, Zeolites 15 (1995) 219 – 227.

[23] G. Xomeritakis, Z. Lai, M. Tsapatsis, Separation of xylene isomers vapors with oriented MFI membranes made by seeded growth, Ind. Eng. Chem. Res. 40 (2001) 544.

[24] M. P. Bernal, J. Coronas, M. Menéndez, J. Santamaría, Characterization of zeolite membranes by temperature programmed permeation and step desorption. J. Membr. Sci. 195 (2002) 125.

[25] S. Mohanty, A.V. McCormick, Prospects for principles of size and shape selective separations using zeolites, Chem. Eng. J. 74 (1999) 1 – 14.

[26] X. Gu, J. Dong, T. M. Nenoff, D. Ozokwelu, Separation of *p*-xylene from multicomponent vapor mixtures using tubular MFI zeolite membranes, J. Membr. Sci. 280 (2006) 624 – 633.

[27] M. Tsapatsis ans Z. Lai, Crystalline membranes, US Patent Application Publication 20050014371A1 (2005).

[28] G. T. P. Mabande, M. Noack, A. Avhale, P. Kolsch, G. Georgi, W. Schwieger, Permeation properties of bi-layered Al-ZSM-5/Silicalite-1 membranes. J. Caro, Micropor. Mesopor. Mater. 98 (2007) 55 – 61.

[29] J. Choi, Sh. Ghosh, L. King, M. Tsapatsis, MFI zeolite membranes from a- and randomly oriented monolayers, Adsorption 12 (2006) 339.

[30] S. Haag, M. Hanebuth, G. T. P. Mabande, A. Avhale, W. Schwieger, R. Dittmeyer, On the use of a catalytic H-ZSM-5 membrane for xylene isomerization, Micropor. Mesopor. Mater. 96 (2006) 168.

Table 1. Characteristics of the exchanged membranes

Membrane	Area x 10^4 [m^2]	Weight gain[a] [mg g^{-1}]	N_2 permeance x 10^8 [mol $s^{-1}m^{-2}Pa^{-1}$][b]	
			Before [c]	After [d]
Na-ZSM-5 (MM-10)	8.90	9.97	5.96 ± 0.23	6.06 ± 0.24
Na-ZSM-5 (MM-16)	8.75	10.08	5.41 ± 0.22	5.54 ± 0.22
Na-ZSM-5 (MM-17)	8.50	9.85	6.12 ± 0.24	6.04 ± 0.23
Na-ZSM-5 (MM-11)	8.72	10.12	6.20 ± 0.24[e]	
Na-ZSM-5 (MM-12)	8.10	9.89	5.78 ± 0.22[e]	
Na-ZSM-5 (MM-13)	7.94	9.35	5.48 ± 0.23[e]	
Na-ZSM-5 (MM-14)	8.21	9.91	5.46 ± 0.21[e]	
Na-ZSM-5 (MM-11)[f]	8.72	10.12		6.28 ± 0.25
Ba-ZSM-5 (MM-11)	8.72	10.12	6.24 ± 0.24[g]	6.31 ± 0.25
Ba-ZSM-5 (MM-14)	8.21	9.91	5.49 ± 0.21[g]	5.51 ± 0.22
Sr-ZSM-5 (MM-12)	8.10	9.89	5.82 ± 0.22[g]	5.91 ± 0.23
Sr-ZSM-5 (MM-16)	8.75[h]	10.08	5.54 ± 0.22[g]	5.56 ± 0.22
Cs-ZSM-5 (MM-13)	7.94	9.35	5.52 ± 0.23[g]	5.52 ± 0.22

[a] After zeolite film deposition

[b] Temperature = 25 ºC, ΔP = 80 kPa

[c] Before xylene permeation measurements

[d] After xylene permeation at 400 ºC

[e] Before ion-exchange

[f] Ba-ZSM-5 back-exchanged with $NaNO_3$

[g] After ion-exchange

[h] The Na-ZSM-5 (MM-16) was exchanged with strontium acetate after the xylene permeation measurements.

Table 2. Elemental composition and depth of the MFI layers.

Membrane	Si/Al[(a)]	M^{n+}/Al %[(a)]	M^{n+}/Al % [(b)]	Thickness (μm)[(c)]
Na-ZSM-5 (MM-10)	12.0	99	-------	20
Na-ZSM-5 (MM-16)	12.6	99	-------	18
Ba-ZSM-5 (MM-11)	11.3	55.0	50	15
Sr-ZSM-5 (MM-12)	14.0	40.3	[(d)]	18
Cs-ZSM-5 (MM-13)	11.6	51.0	57	15

[(a)] Measured by atomic absorption in the zeolite powder

[(b)] Determined by EPMA in the MFI film.

[(c)] Measured in the SEM micrographs

[(d)] No value given because the Sr line overlaps with the Si signal.

Table 3. Permeation fluxes of individual xylene isomers and ideal selectivities

Membrane	Permeation flux x 10^5 [mol $s^{-1}m^{-2}$][a]			Ideal selectivity	
	p-xylene	*m*-xylene	*o*-xylene	p/m	p/o
Na-ZSM-5 (MM-10)	5.10	0.95	0.81	5.41	5.62
Ba-ZSM-5 (MM-11)	4.97	0.62	0.41	8.12	12.12
Sr-ZSM-5 (MM-12)	3.22	0.68	0.48	4.73	6.74
Cs-ZSM-5 (MM-13)	3.13	0.58	0.39	5.39	8.02

[a] Temperature = 370 ºC. Feed partial pressure: 2.026 kPa *p*-xylene, 1.92 kPa *m*-xylene and 1.52 kPa *o*-xylene.

Table 4. N_2 permeance and weight loss of the sandpapered membrane.

Membrane	N_2 permeance x 10^8 [mol s^{-1} m^{-2} Pa^{-1}]	Permeance increase [%]	Weight loss [a] [mg/g]	Weight loss % [b]
Na-ZSM-5[c]	5.96	-----	----	----
1º [d]	7.41	24.3	0.76	9.63
2º [d]	8.11	36.1	2.59	32.82
3º [d]	8.75	46.8	5.05	64.00

[a] Weight gain of the calcined membrane 7.89 mg/g

[b] Calculated with respect to the total weight gain

[c] After calcination

[d] After each sandpaper step

Table 5. Physicochemical properties of the cations exchanged.

Cation	Ionic radio [Å]	(z*e)/radio [C/ Å]	Pauling Electronegativity
Na^{+}	1.16	1.38×10^{-19}	0.93
Cs^{+}	1.84	8.71×10^{-20}	0.79
Ba^{2+}	1.43	2.15×10^{-19}	0.89
Sr^{2+}	1.27	2.52×10^{-19}	0.95

Table 6. Comparison with literature data reported for MFI-type composite membranes

Support	Zeolite film	Feed (kPa)			Max. T	Permeance $_{p\text{-xylene}}$	p/o[a]	Reference
		p-xylene	*o*-xylene	*m*-xylene	(ºC)	x 10^7 [mol s^{-1} m^{-2} Pa^{-1}]		
α-Al_2O_3[b]	Silicalite	0.27	0.59	-----	390	3.00	16.0	[1]
α-Al_2O_3[b]	H-ZSM-5 (60)[e]	0.50	0.50	-----	200	0.40	6.0	[28]
α-Al_2O_3[c]	Silicalite	1.50	1.35	4.50	400	0.01	7.0	[2]
α-Al_2O_3[c]	Silicalite	0.26	0.2	0.49	300	0.10	10.0	[26]
SS[c]	H-ZSM-5[d] (600)[e]	2.10	2.10	-----	237	0.05	2.8	[3]
SS[c]	Na-ZSM-5 (100)[e]	0.23	0.26	0.83	400	0.51	4.4	[14]
SS[c]	Na-ZSM-5 (11.3)[e]	0.23	0.26	0.83	400	0.62	3.9	This work
SS[c]	Ba-ZSM-5 (11.3)[e]	0.23	0.26	0.83	400	0.54	8.4	This work

[a] Separation factor (measured at the maximum temperature)

[b] Disc

[c] Tubular support

[d] Boron-substituted

[e] Si/Al ratio

Figure legends

Figure 1. Schematic diagram of the shell-and-tube membrane module used in xylene permeation measurements.

Figure 2. X-ray diffraction patterns of the Na-ZSM-5 powder as synthesized with different Si/Al ratios (100 and 14).

Figure 3. X-ray patterns of the composite Na-ZSM-5 membranes before being exchanged with Ba, Cs and Sr.

Figure 4. SEM top views of the surface of (a) the silicalite seeded SS support and of the Na-ZSM-5 membrane after (b) the first synthesis, (c) the third, and (d) xylene measurements.

Figure 5. Extent of the zeolite layer grown inside the support: (a) SEM profile, (b) EPMA composition.

Figure 6. N_2 permeance as a function of the *p*-xylene activity (p/p_S). * Percentage of flux through non-zeolitic pores.

Figure 7. Effect of the temperature on ternary xylene mixture permeation fluxes and separation factors through the Na-ZSM-5 (MM-10), Ba-ZSM-5 (MM-11), Cs-ZSM-5 (MM-13) and Sr-ZSM-5 (MM-12) membranes. Feed partial pressures: 0.23 kPa *p*-xylene, 0.83 kPa *m*-xylene, 0.26 kPa *o*-xylene.

Figure 8. Reproducibility of the xylene permeation fluxes in ternary mixtures and separation factors at 370 ºC for the Na, Ba and Sr-ZSM-5 membranes. Feed partial pressures: 0.23 kPa *p*-xylene, 0.83 kPa *m*-xylene, 0.26 kPa *o*-xylene. * Ba-ZSM-5 (MM-11) back-exchanged with $NaNO_3$.

Figure 9. Similar trends in both separation factors and ideal selectivities at 370ºC.

Figure 10. Comparison of our data with published results: p/o separation factor vs. *p*-xylene permeance for MFI membranes.

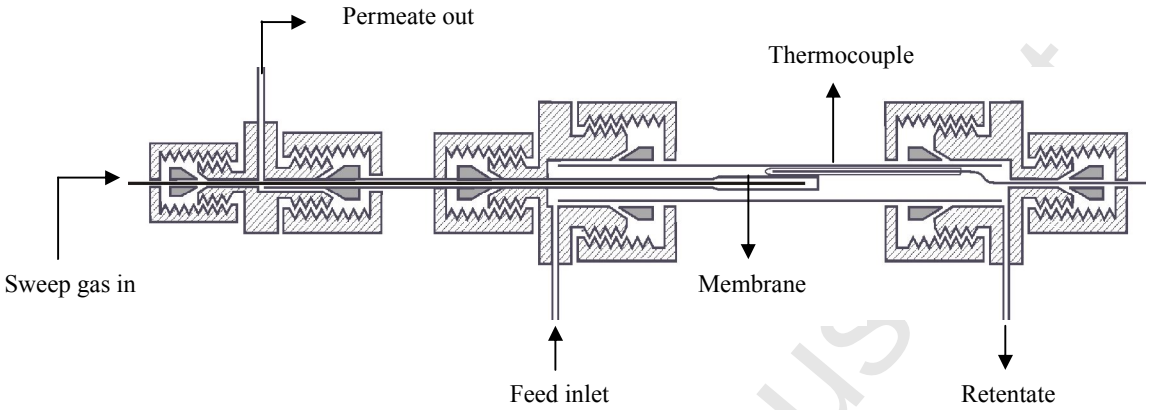

Fig. 1

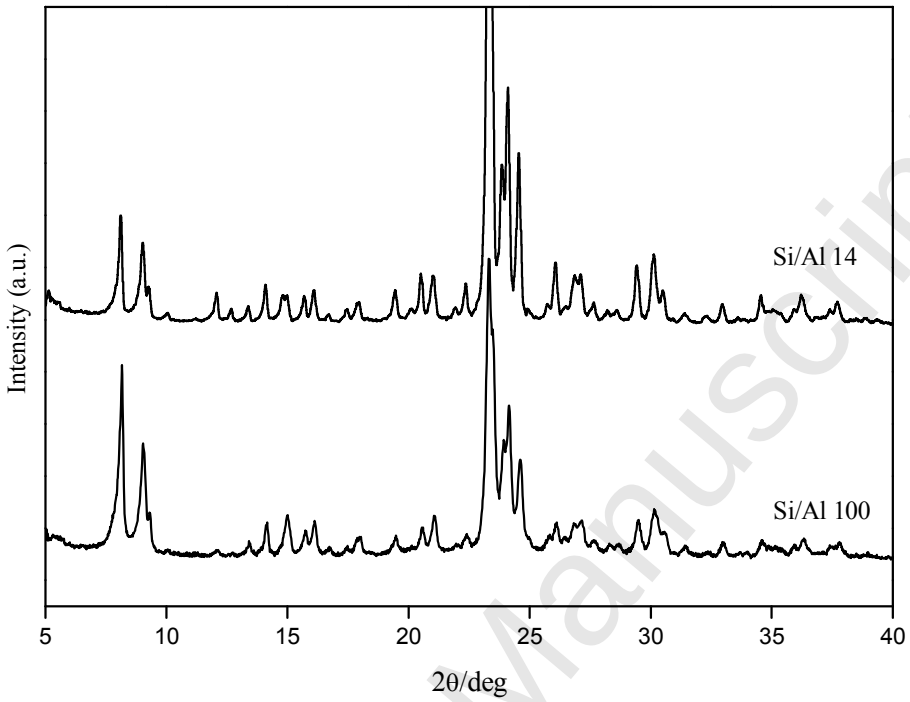

Fig. 2

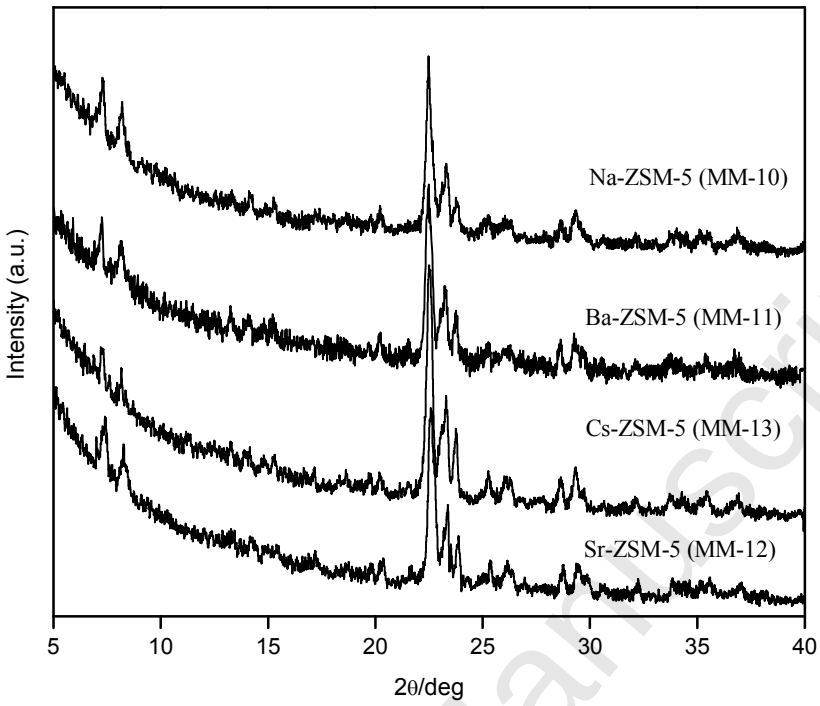

Fig. 3

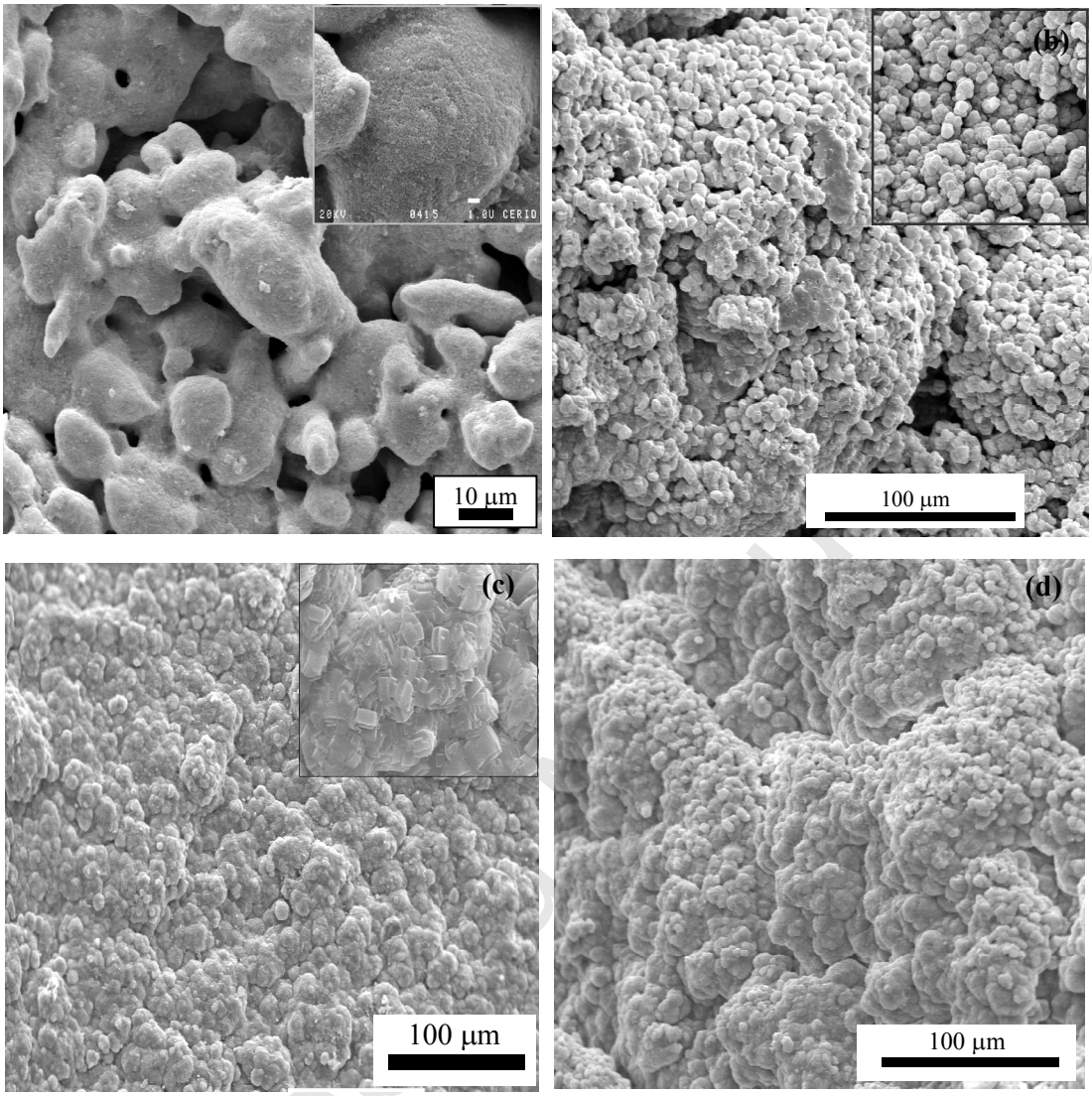

Fig. 4

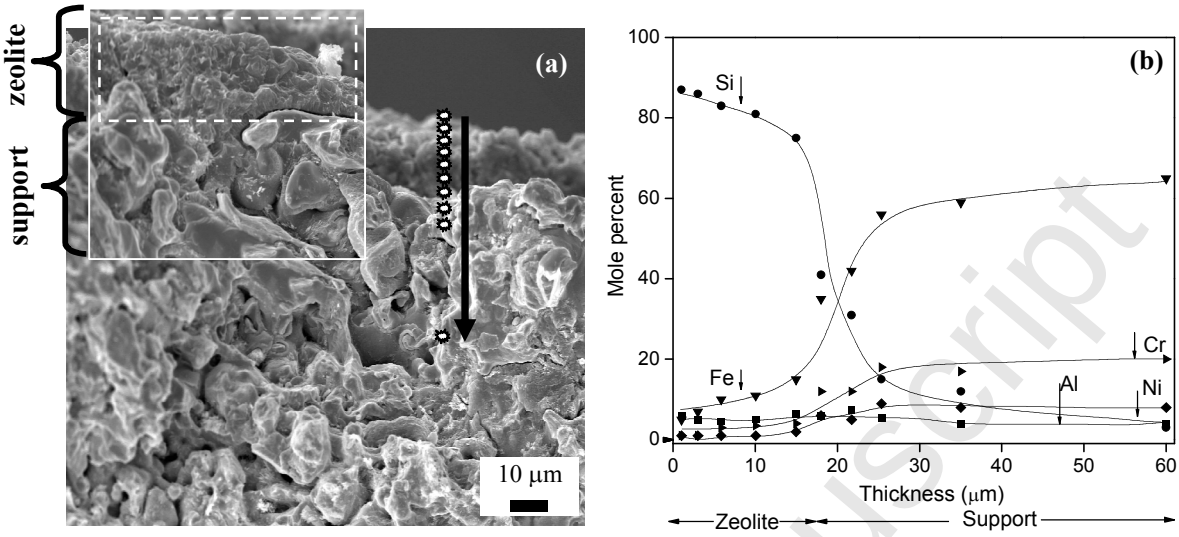

Fig. 5

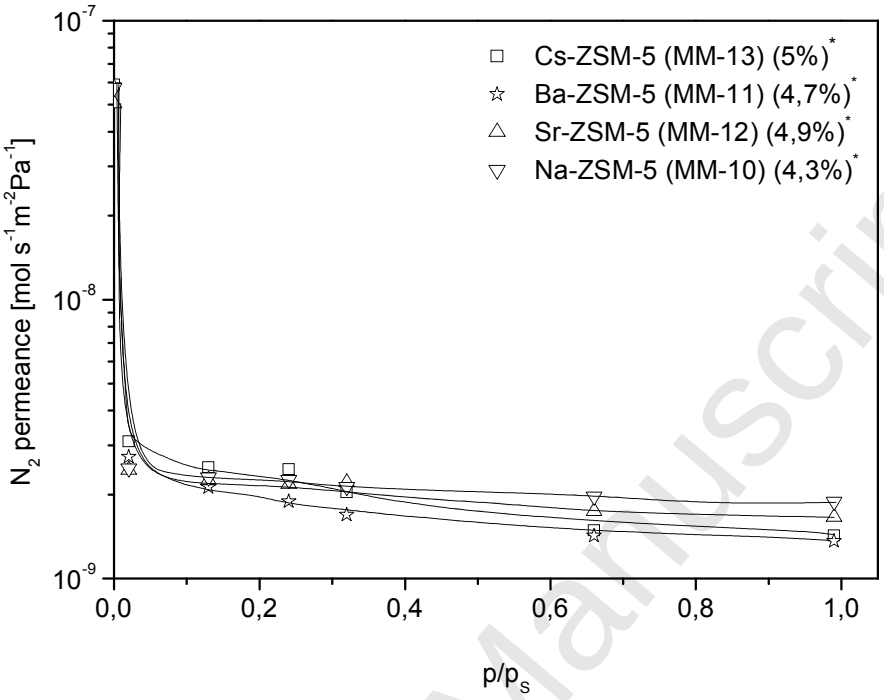

Fig. 6

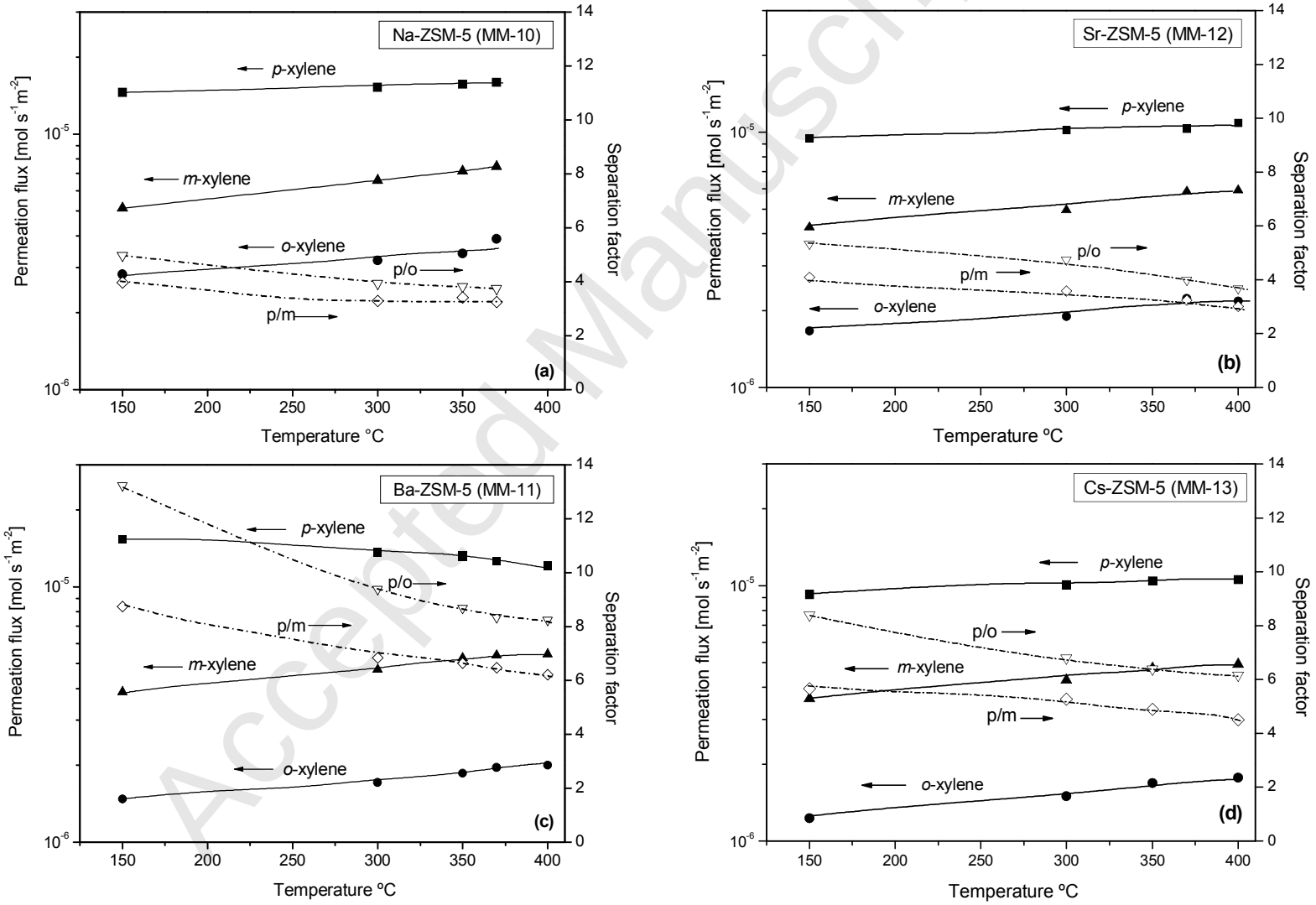

Fig. 7

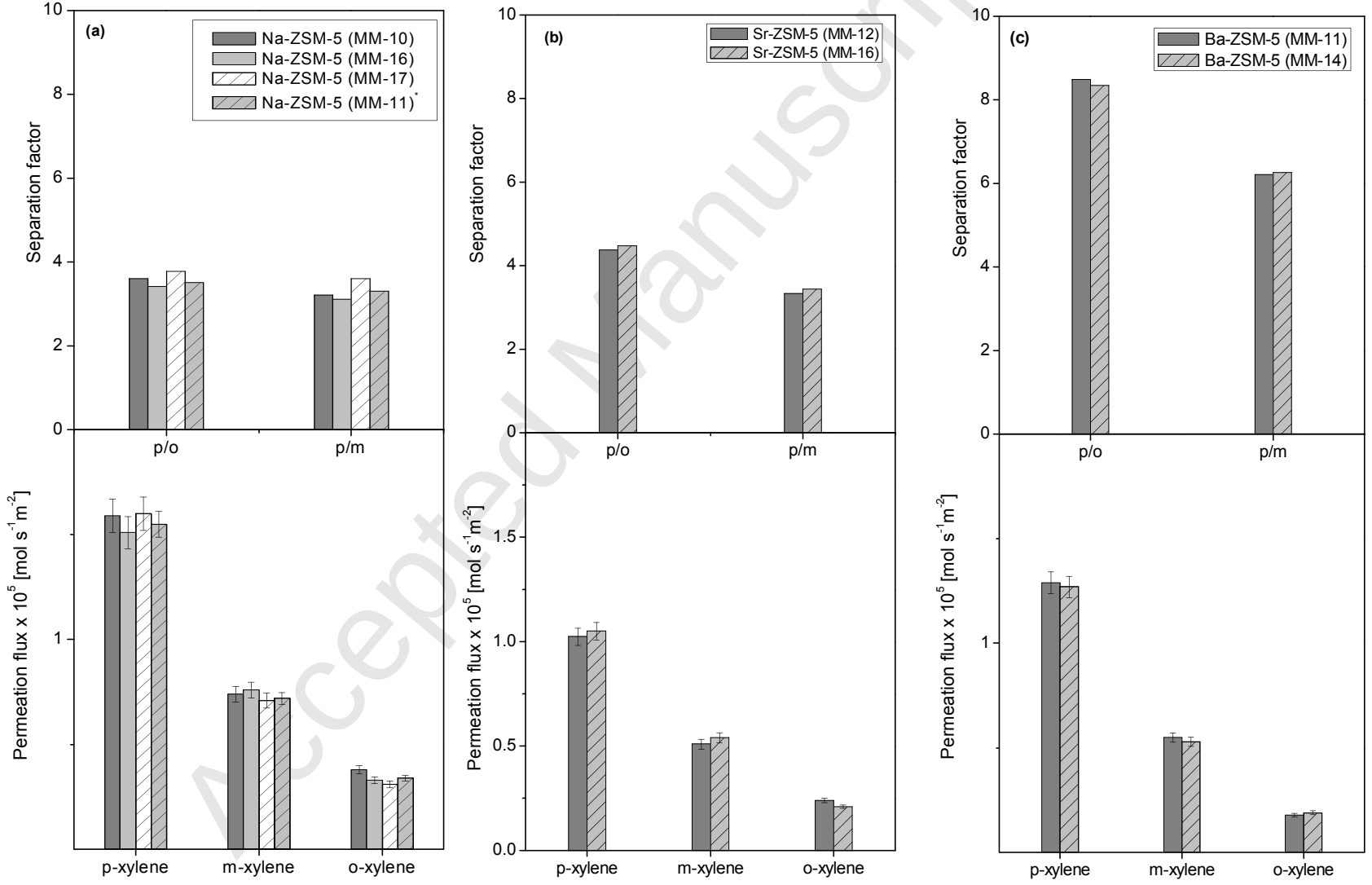

Fig. 8

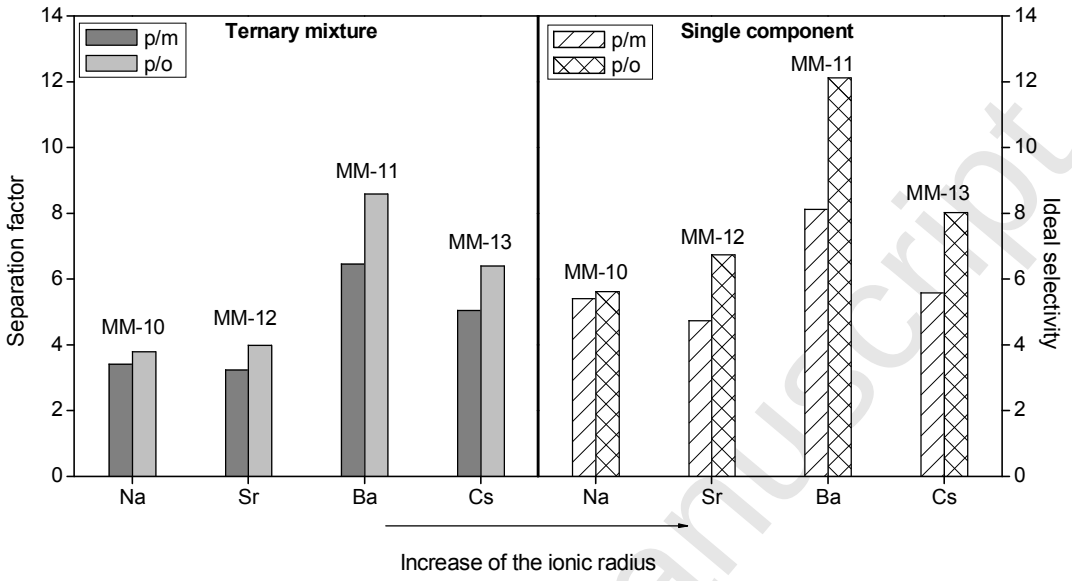

Fig. 9

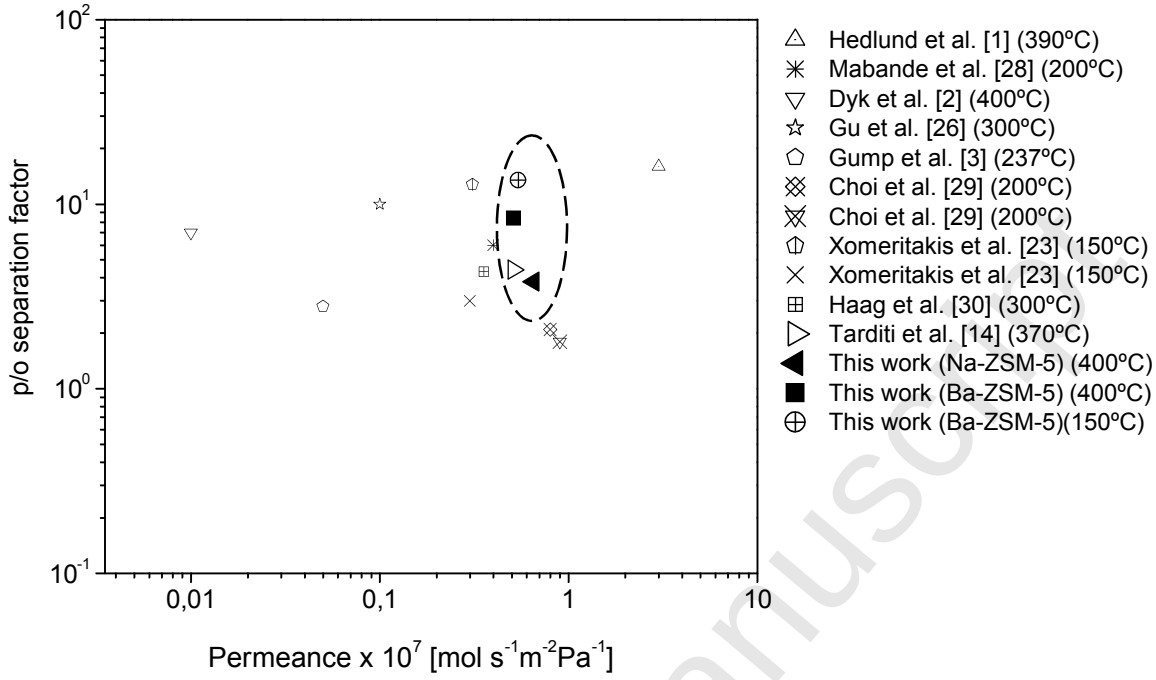

Fig. 10